Z. Phys. B 104, 475–479 (1997)

ZEITSCHRIFT FÜR PHYSIK B

Vibrational spectroscopy of indium-doped $Pb_{0.9}Mn_{0.1}Te$ alloy

N. Romčević[1], Z.V. Popović[1], D.R. Khokhlov[2], I.I. Ivanchik[2], A.V. Nikorich[3], W. König[4]

[1] Institute of Physics, P.O. Box 57, YU-11001 Belgrade, Yugoslavia
[2] Low-Temperature Physics Department, Moscow State University, 117234 Moscow, Russia
[3] Applied Physics Institute of the Moldavian Academy of Science, Kishenev, Moldavia
[4] Max-Planck-Institut für Festkörperforschung, Heisenbergstrasse 1, D-70569 Stuttgart, Germany

Received: 5 November 1996 / Revised version: 15 April 1997

Abstract. Raman scattering and far-infrared reflection spectra of 0.5 at.% In doped $Pb_{0.9}Mn_{0.1}Te$ single crystal at temperatures between 10 and 300 K are presented. The infrared spectra have been fitted using a modified plasmon-phonon interaction model with an additional oscillator (at about 122 cm^{-1}) representing a local In-impurity mode. Phonons in this mixed crystal exhibit intermediate mode behavior. The plasma frequency decreases on cooling from 300 to 25 K and increases sharply between 20 and 10 K. The results of galvanomagnetic measurements are also presented.

PACS: 63.20.Pw; 78.50.Ge; 72.15.Gd; 71.28.+d

1. Introduction

The properties of $A^{IV}B^{VI}$ semiconductor alloys doped with group III elements (In, Ga, Tl) have been intensively studied during the past two decades [1–4]. Particularly, the behavior of indium in these alloys has been studied in much detail because doping with indium results in the appearance of a persitent photoconductivity effect, together with a series of other interesting features [5, 6]. In this work, we concentrate on the effect of indium on the optical and transport properties of $Pb_{1-x}Mn_xTe$ mixed crystals.

The properties of $Pb_{1-x}Mn_xTe$ alloys are not very well known. Increasing the MnTe amount in $Pb_{1-x}Mn_xTe$ mixed crystal leads to the energy gap increasing according to $\partial E_g/\partial x$ = (38 ÷ 48) meV/mol% MnTe [7]. Concerning the electronic spectrum, $Pb_{1-x}Mn_xTe$(In) is quite similar to that of $Pb_{1-x}Sn_xTe$(In) and the Fermi level is pinned within the gap for $x > 0.05$ [7]. Finally, when doped with indium this alloy shows a persistent photoconductivity effect.

In a previous series of papers [8–10], the existence of an In-impurity mode was confirmed at about 122 cm^{-1} in the IR-spectra of $Pb_{0.75}Sn_{0.25}Te$(In) alloy [8, 9] and at about 115 cm^{-1} in the Raman spectra of PbTe(In) crystal [10]. This mode is connected with metastable electronic impurity states which are responsible for the appearance of the persistent photoconductivity effect. By expanding this study to the $Pb_{0.9}Mn_{0.1}Te$(In) system, we expect to confirm our previous conclusions, and get a more uniform picture of the In-impurity states in the series of lead-telluride based alloys.

In this work, we present the results of a far-infrared reflection and Raman scattering examination of indium-doped lead-manganese-telluride completed by galvanomagnetic measurements. The far-infrared spectra have been fitted using a modified plasmon-phonon interaction model with an extra oscillator. It describes the local In-impurity mode and represents the population of metastable states. The phonon properties of the lead-manganese-telluride alloys, and their intermediate mode behavior, are also discussed. Finally at $T < 25$ K due to the persistent photoconductivity effect we observed a difference in the electrical resistivity (galvanomagnetic measurements) illuminated and unilluminated $Pb_{0.9}Mn_{0.1}Te$(In) sample.

2. Experimental

The sample under investigation was a $Pb_{0.9}Mn_{0.1}Te$ single crystal, doped with 0.5 at.% In and grown using the Bridgeman technique. The indium impurity was introduced into the liquid zone as already described [7]. For x = 0.1, the Fermi level was pinned in the forbidden band.

A Bruker IFS 113v spectrometer, with an Oxford model cryostat, was used for the low-temperature far-infrared reflection measurements.

The transport parameters were obtained by measuring the Hall effect in the Van der Pauw geometry. The samples were held in a close-cycle helium cryostat, the magnetic field strength was B = 0.45 T and the current through the sample was I = 10 mA.

The Raman spectra were excited using the 488 nm line of an argon ion laser. The average power was about 100 mW. The monochromator was a Jobin-Yvon model U-1000 with 1800 grooves/mm-holographic gratings. As a detector, we used a Peltier-cooled RCA 31034A photomultiplier with a conventional photon-counting system. The samples were held in a closed-cycle cryostat, equipped with a low-temperature controller and evacuated by a turbopump.

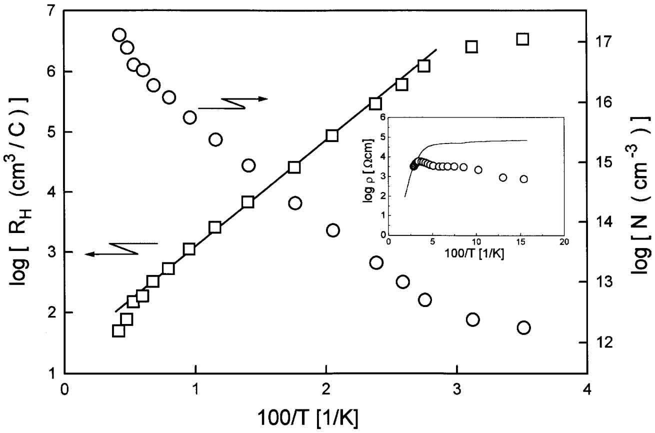

Fig. 1. Temperature dependence of the $Pb_{0.9}Mn_{0.1}Te(In)$ Hall coefficient (R_H) and free carrier concentration (N). *Inset:* Change of specific electrical resistivity vs. temperature for the unilluminated (solid line) and illuminated (open circles) $Pb_{0.9}Mn_{0.1}Te(In)$ single-crystal sample

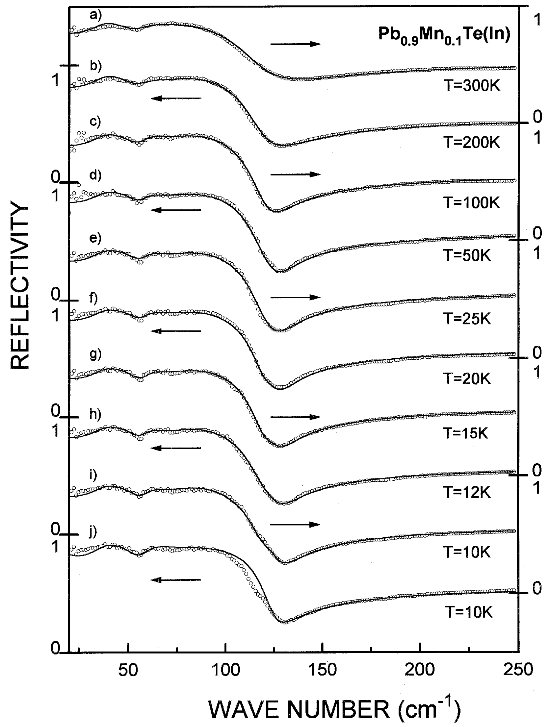

Fig. 2. Far-infrared reflectivity spectra of $Pb_{0.9}Mn_{0.1}Te(In)$ single crystal measured at different temperatures. The experimental spectra are represented by circles. The solid lines are calculated spectra obtained by using fitting procedure based on the model given by (1). All the parameter values have been given in Table 1. For T = 10 K, the calculated spectra are given with (i) and without (j) additional oscillator at 122 cm^{-1}

3. Results and discussion

The specific electrical resistivity vs. temperature of $Pb_{0.9}Mn_{0.1}$ Te(In) is shown in Fig. 1 (inset). The line and dots represent the unilluminated and low-intensity infrared radiation illuminated values, respectively. A difference between these resitivity curves appears when $T < 25$ K, as a consequence of the persistent photoconductivity effect [5, 8]. This effect is considerably lower than previously found in the case of $Pb_{1-x}Sn_xTe(In)$ alloys. Dependencies of the Hall constant (R_H) and free carrier concentration (N) on the temperature, for an unilluminated $Pb_{0.9}Mn_{0.1}Te(In)$ sample, are shown in Fig. 1. The activation part of $R_H(T)$, shown by the solid line in Fig. 1, gives the value of activation energy of E_a = 67 meV.

The far-infrared reflection spectra of 0.5 at.% In-doped $Pb_{0.9}Mn_{0.1}Te$ are given by the points in Fig. 2a–j. The lines were obtained using a modified plasmon-phonon interaction model:

$$\varepsilon = \varepsilon_\infty \left(\prod_{j=1}^{3} \frac{\omega_{j\mathrm{LO}}^2 - \omega^2 + i\gamma_{j\mathrm{LO}}\omega}{\omega_{j\mathrm{TO}}^2 - \omega^2 - i\gamma_{j\mathrm{TO}}\omega} - \frac{\omega_p^2}{\omega(\omega + i\tau^{-1})} + \frac{\omega_{\mathrm{LOC}}^2}{\omega_0^2 - \omega^2 + iG\omega} \right) \qquad (1)$$

where ω_{TO}, ω_{LO} and ω_{P} are transverse, longitudinal and plasma frequencies, respectively. γ_{TO} and γ_{LO} are the damping of TO and LO modes, τ is the free-carrier relaxation time and ε_∞ is the high frequency dielectric constant. The first term in (1) comes from the lattice vibration contribution to the dielectric constant. The second term comes from the free carrier contribution to the dielectric constant. The third term represents the In-impurity local mode, where ω_0 is the characteristic frequency, G is the damping and ω_{LOC}^2 is the "strength" of the oscillator. The fitting procedure is the same as the one applied to $Pb_{0.75}Sn_{0.25}Te(In)$ [8]. The best fit parameters have been listed in Table 1.

The values of ω_{P} and τ^{-1} vs. temperature (see Table 1) are in qualitative agreement with literature data for ω_{P} and τ^{-1} in other In-impurity doped lead-telluride based alloys [8, 9] where the Fermi level is pinned in the gap. Typically, ω_{P} drops from 89 cm^{-1} (T = 300 K) to 75 cm^{-1} (T = 25 K) and, then, increases rapidly as the temperature decreases. Similary τ^{-1} drops from 111 cm^{-1} (300 K) to 53 cm^{-1} (25 K), while a slight increase to 56 cm^{-1} (10 K) is observed with a further temperature decrease. Such ω_{P} and τ^{-1} behaviors are a consequence of the persistent photoconductivity effect, already seen in galvanomagnetic measurements.

The oscillators indexed $i = 1, 2$ (Table 1) can be identified as PbTe and MnTe-like lattice vibration modes in the $Pb_{1-x}Mn_xTe$ (x = 0.1) mixed crystal. They are the dominant structures in the far-infrared reflection spectra (Fig. 2). At T = 300 K, the corresponding PbTe and MnTe TO/LO mode pairs are (37/50) cm^{-1} and (59/107) cm^{-1}, respectively (see Table 1).

The weak intensity oscillator at 70 cm^{-1} (indexed i = 3 in Table 1) is an edge Brillouin zone mode (the density of states of PbTe [11] has a maximum at about this frequency) which becomes infrared active due to impurity induced disorder. This mode has been already observed in many PbTe based alloys [9, 12].

Unpolarized Raman scattering spectra of $Pb_{0.9}Mn_{0.1}Te$ (In) measured in the spectral range 40–200 cm^{-1} at temperatures 300 and 10 K are shown in Fig. 3. The room temperature spectrum is similar to most previously published Raman spectra for PbTe-based alloys [13, 14]. It is characterized by two strong peaks, at about 125 cm^{-1} and 143 cm^{-1}, which originate from the TeO_2 lattice vibrations. This is because TeO_2 thin layer is formed on the surface of the sample [15].

Table 1. Optical parameters (in $\mathrm{cm^{-1}}$) of plasmons and phonons obtained by oscillator fitting of the $Pb_{0.9}Mn_{0.1}Te(In)$ reflection spectra

T	ω_{jTO}	ω_{jLO}	γ_{jTO}	γ_{jLO}	ω_P	ε_∞	τ^{-1}	ω_0	ω_{LOC}	G
10	37 60 78	54 107.4 70	9 10 27	12 13 37	77.7	54	56	122	27.9	29
12	37 60 78	54 107.2 70	9 10 27	12 13 37	76.6	54	55.4	122	27.9	29
15	37 60 78	54 107 70	9 10 27	12 13 37	76.4	54	54.6	122	27.9	28
20	37 59 78	54 107 70	9 10 31	12 13 41	75.7	54	52.7	122	27.75	28
25	37 59 78	54 107 70	9 9 31	12 12 41	75.5	53	52.6	122	27.65	28
50	37 59 78	54 107 70	9 10 31	12 10.3 41	76.9	52	59.5	122	26.2	28
100	37 59 78	53.5 107 70	9 10 31	14 8.2 41	77	51	71.4	122	24	28
200	37 59 77	52 107 70	9 16 35	14 9.3 51	82	50	83.3	122	22.9	28
300	37 59 76	50 107 70	9 16 44	18 16 53	89	50	111	122	21.6	28

When the temperature is lowered to 10 K, the frequency of the two modes shift toward higher wave numbers. Also, two additional modes of weak intensity, at about $53\,\mathrm{cm^{-1}}$ and $108\,\mathrm{cm^{-1}}$, appear. The frequency position of these modes is obtained by using a deconvolution technique. The accuracy of the method is about $\pm 1\,\mathrm{cm^{-1}}$.

Assignment of the vibrational modes observed in Figs. 2 and 3 can be made on the basis of the phonon properties of mixed crystals [16]. The Raman (□) and far-infrared (×) optical mode frequencies for $Pb_{0.9}Mn_{0.1}Te$, together with the literature values (○) for PbTe [17] and MnTe [18] are shown in Fig. 4. The solid lines represent a linear interpolation of the experimental data. The results shown in Fig. 4 suggest more an intermediate one-mode/two-mode behavior of this mixed crystal rather than a real two-mode behavior.

Indeed, for $x \to 0$ there are the TO and LO modes of PbTe and the band mode I_{Mn}. As x is increased, the band mode splits into the longitudinal mode LO_2 and the transverse mode TO_1. The vibrational modes that evolve from the LO and TO phonons of PbTe are designated as LO_1 and TO_2. As $x \to 1$, the LO_1 mode which is the LO phonon of PbTe, evolves into the LO mode of MnTe. The TO_1 phonon which evolves from the impurity mode I_{Mn}, becomes the TO vibrational mode of MnTe. The two remaining phonons, TO_2 and LO_2, merge to become the impurity band of Pb in the MnTe. Taking the MnTe force constant from [18] we calculated a frequency of I_{Pb} mode of $91\,\mathrm{cm^{-1}}$. This value is very close to the value obtained by linear extrapolation ($100\,\mathrm{cm^{-1}}$), Fig. 4. This strongly supports the phonon picture given in Fig. 4.

The temperature change of ε_∞ is shown in the inset of Fig. 4. Decreasing the temperature increases ε_∞. This is in agreement with the theoretical predictions given in [19] for a cubic crystal without phase transformation. Also the relatively high values of ε_∞ given in Table 1 are typical for this kind of material [8, 17, 19].

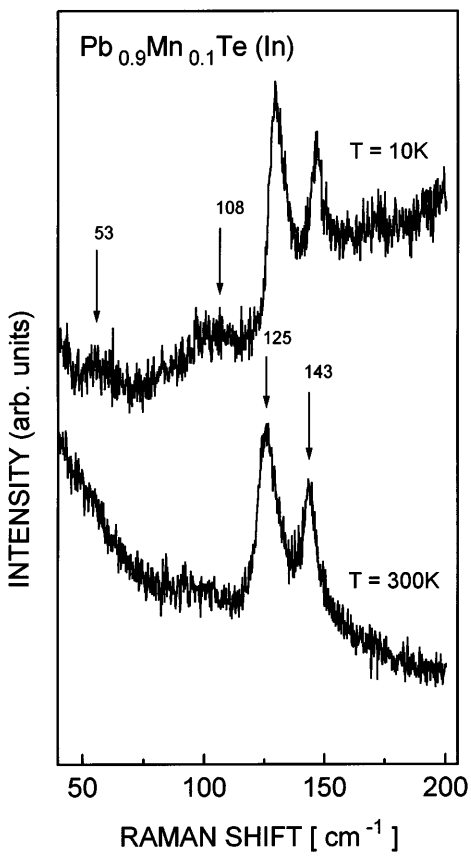

Fig. 3. Unpolarized Raman scattering spectra of $Pb_{0.9}Mn_{0.1}Te(In)$ measured at 300 at 10 K

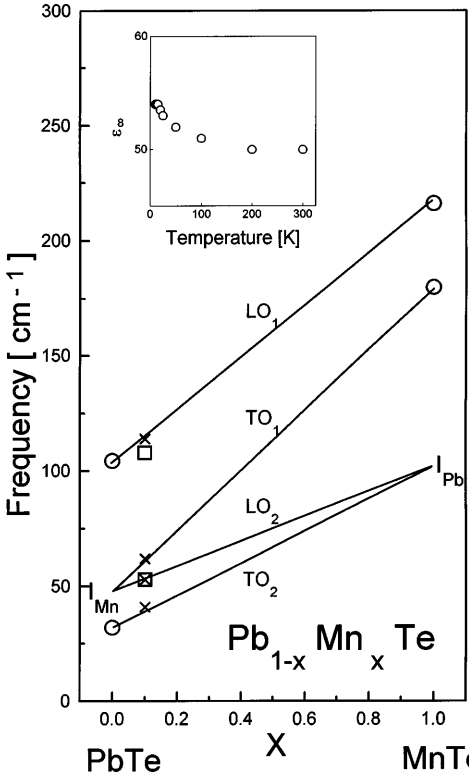

Fig. 4. Concentration dependence of the optical mode frequencies of $Pb_{1-x}Mn_xTe(In)$ single crystal. $\times(\square)$ – IR (Raman) measurement of $Pb_{0.9}Mn_{0.1}Te(In)$; $\circ$ – [17]. The solid line is a linear interpolation. *Inset:* $Pb_{0.9}Mn_{0.1}Te(In)$ high frequency dielectric constant (ε_∞) vs temperature. The dashed line is a guide for eye

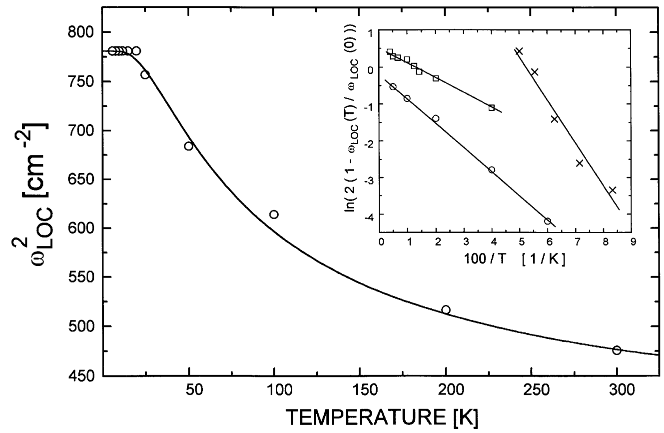

Fig. 5. Temperature dependence of the additional oscillator "strength" (ω^2_{LOC}). The solid line is calulated by (2). *Inset:* The $\ln((2(1 - \omega^2_{\mathrm{LOC}}(T)/\omega^2_{\mathrm{LOC}}(0)))$ vs $100/T$ dependence for $Pb_{0.9}Mn_{0.1}Te(In)$ – $\circ$; $PbTe(G)$ – $\square$, and $Pb_{0.75}Sn_{0.25}Te(In)$ – $\times$. The solid lines are linear interpolations

Let us return again to Fig. 2. A weak structure is noticeable at T = 50 K and, by further temperature lowering, at $T < 25$ K a saddle hump at about $\omega_0 = 122\,\mathrm{cm}^{-1}$ is clearly observed. In order to obtain agreement between the measured and the calculated spectra, an oscillator of characteristic frequencey ω_0, was added to (1). G is the damping and ω^2_{LOC} the "strength" of this oscillator. A similar structure has been observed in the far-infrared reflection spectra of $Pb_{0.75}Sn_{0.25}Te(In)$ [8, 9], PbTe(In) [10] and of PbTe(Ga) [20], but the additional structure in $Pb_{0.9}Mn_{0.1}Te(In)$ is less pronounced. This is a consequence of the weak intensity of the persistent photoconductivity effect.

In order to demonstrate the existence of an additional mode at about $122\,\mathrm{cm}^{-1}$, the calculated spectra with and without this oscillator are shown in Fig. 2i and j. Significant disagreement between the calculated and the experimental data in Fig. 2j led us to conclude that in $Pb_{0.9}Mn_{0.1}Te(In)$, like many other Indium doped PbTe-based alloys [8–10], the mode at $122\,\mathrm{cm}^{-1}$ really exists.

The temperature dependence of oscillator strength ω^2_{LOC} is shown in Fig. 5. The strength of the additional oscillator above T = 25 K decreases sharply by increasing the temperature. As previously discussed [8–10, 20], the far-infrared reflection spectra of lead telluride-based alloys doped with indium or gallium have quite similar features. In every case an additional structure is observed. The strength of this oscillator strongly decreases when the temperature is raised above the critical one where the persistent photoconductivity effect is registered (T_c = 25 K for $Pb_{1-x}Sn_xTe(In)$ [8] and $Pb_{0.9}Mn_{0.1}Te(In)$ [7], and 80 K for PbTe(Ga) [21]). The oscillator strength in $Pb_{0.75}Sn_{0.25}Te(In)$ drops so rapidly that at $T > T_c$ [9] the additional oscillator in the reflection spectra completely disappears. Because this oscillator appears in the IR spectra of $Pb_{0.9}Mn_{0.1}Te(In)$, $Pb_{0.75}Sn_{02.5}Te(In)$ and PbTe(In) at the same frequency it led us to conclude that these structures are of the same origin.

One can see, however, that the oscillator frequency appears at about $122\,\mathrm{cm}^{-1}$ for both $Pb_{0.9}Mn_{0.1}Te(In)$ and $Pb_{0.75}Sn_{0.25}Te(In)$ despite the fact that their electronic energy spectra are quite different. Indeed, the galvanomagnetic measurements show that the Fermi level pinning position is about 20 meV below the bottom of conduction band for $Pb_{0.75}Sn_{0.25}Te(In)$ [5] and only about 12 meV for $Pb_{0.9}Mn_{0.1}Te(In)$ [7]. Measurements of the localization effect in strong magnetic fields have shown that the energy separation of the ground and the metastable impurity states is also quite different for these two cases [22]. Accordingly, since this oscillator appears in the In-doped IV-VI alloys at the same energy, we concluded that this mode is a local mode, originating from the In-impurity, as discussed in detail in [10].

On the other hand, because the strength of this oscillator rises sharply at temperature lower than 25 K, we conclude that this mode represents a population of metastable In-impurity states due to the transfer of electrons from two-electron to one-electron impurity states.

The strong temperature dependence of the occupancy of the metastable impurity states may result from a range of mechanisms. Let us assume first that the respective energy position and the barrier (E_b) separating the ground and metastable impurity states do not change with temperature, and that there is no dispersion of the metastable impurity state energies.

The occupancy of these states is defined by the balance of the photo-excitation and recombination. The excitation rate does not change with temperature. Let us assume that the main mechanism of recombination, at least at temperatures close to and above T_c, is thermal excitation over the

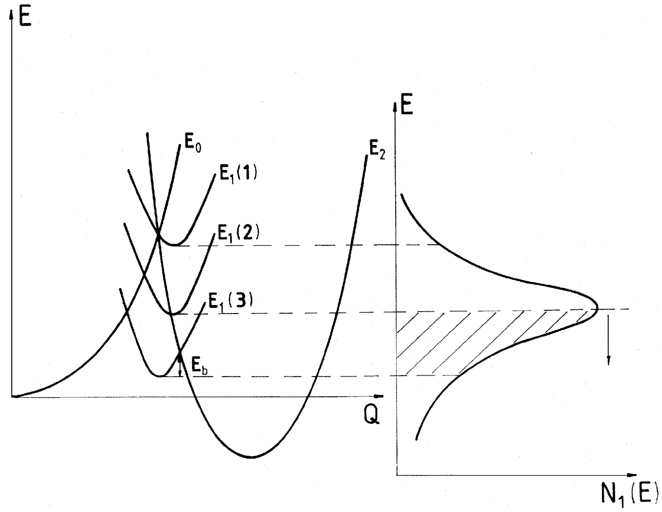

Fig. 6. Configuration-coordinate diagram of the system corresponding to $T = T_c = 25\,$K. The curves E_i ($i = 0, 1, 2$) correspond to the states with i electrons localized on the impurity center. E_b – barrier between the ground two-electron and metastable one-electron states. *Inset:* the profile of the density of states of a metastable impurity state E_1. The curves $E_1(j)$ correspond to the different positions in the density of state profile. $T = T_c$ corresponds to the formation of a barrier E_b at the maximum of E_1 density of states. The states E_1 for which there exists a barrier E_b are filled. The energy of the metastable states decreases when the temperature is lowered (the arrow near the density of states profile)

barrier E_b (see Fig. 6). It is easy to show that the excitation probability is

$$W = 0.5 \exp(-E_b/kT) .$$

Then, the temperature dependence factor of the metastable impurity states occupancy is proportional to $(1 - W)$. Thus,

$$\omega^2_{\mathrm{LOC}}(T) = \omega^2_{\mathrm{LOC}}(0)(1 - 0.5 \exp(-E_b/kT)) . \qquad (2)$$

One can see that (2) fits the experimentally measured values of $\omega^2_{\mathrm{LOC}}(T)$ quite well (a solid line in Fig. 5). Using (2), we obtain $E_b = 6\,$meV. The obtained results for E_b of $Pb_{0.9}Mn_{0.1}Te$ doped with 0.5 at.% In is between the values found for PbTe(Ga) ($E_b = 3\,$meV) and $Pb_{0.75}Sn_{0.25}Te$(In) ($E_b = 10\,$meV) which is shown in the inset of Fig. 5.

Another possible mechanism accounting for the change of the metastable impurity state occupancy is the shift of this state in the configuration-coordinate space with temperature. One can expect a considerable dispersion of the metastable impurity state energy, as evidenced by the galvanomagnetic data for $Pb_{0.75}Sn_{0.25}Te$(In) [3, 5]. Then, if we do not take into account the thermally activated processes, the rapid change in the oscillator strength at $T = (20–30)\,$K corresponds to the disappearance of a barrier between the metastable and the ground impurity states for the peak of the E_1 density of state (see Fig. 6). The main advantage of the presented picture, in contrast to the previous mechanism, is a clear physical interpretation of T_c as the temperature below which the main part of the metastable impurity states becomes populated in non-equilibrium conditions. However, it seems likely that both mechanisms are involved in the effect, and the experimental data available do not allow the conclusion as to which one gives the main contribution.

4. Conclusion

Raman scattering, far-infrared reflection as well as galvanomagnetic measurements were performed on an In doped $Pb_{0.9}Mn_{0.1}Te$ single crystal in the temperature range 10–300 K. The persistent photoconductivity effect produces a decrease of electrical resistivity and plasma-edge shift at $T < 25\,$K. The intermediate one-mode/two-mode behavior of the optical modes is seen in Raman and far-infrared measurements. A new structure in the far-infrared reflection spectra was fitted with an additional oscillator. This mode is assigned to a loocal In-impurity mode and represents a population of metastable states due to the transfer of electrons from two-electron to one-electron metastable impurity states.

This work was supported by the Serbian Ministry of Science and Technology under Project No. 01E09.

References

1. Akimov, B.A., Dmitiriev, A.V., Khokhlov, D.R., Ryabova, L.I.: Phys. Status Solidi (a) **137**, 9 (1993)
2. Vul, M., Voronova, I.D., Kalyuzhnayz, G.M., Mamedov, T.S., Ragimova, T.Sh.: Zh. Eksp. Teor. Fiz. Pis. Red. **29**, 21 (1979) [Engl. Trans JETP Lett. **29**, 18 (1979)]
3. Akimov, B.A., Brandt, N.B., Klimonskiy, S.O., Ryabova, L.I., Khoklov, D.R.: Phys. Lett. A **88**, 483 (1982)
4. Akimov, B.A., Khokhlov, D.R.: Semicond. Sci. Technol. **8**, 349 (1993)
5. Akimov, B.A., Ryabova, L.I., Ytasenko, O.B., Chudinov, S.M.: Fiz. Tekh. Poluprov. **13**, 752 (1979) [Engl. Trans. Sov. Phys. Semicond. **13**, 441 (1979)]
6. Zasavitskiy, I.I., Matveenko, A.B., Matsonashvili, B.N., Trofimov, V.T.: Fiz. Tekh. Poluprovodn. **21**, 1789 (1987) [Engl. Trans. Sov. Phys. Semicond. **21**, 1084 (1987)]
7. Akimov, B.A., Nikorich, A.V., Ryabova, L.I., Shirokiva, N.A.: Fiz. Tekh. Poluprovodn. **23**, 1019 (1989) [Engl. Trans. Sov. Phys. Semicond. **23**, 748 (1989)]
8. Romčević, N., Popović, Z.V., Khokhlov, D.R., Nikorich, A.V., König, W. Phys. Rev. B **43**, 6712 (1991)
9. Romčević, N., Popović, Z.V., Khokhlov, D.R.: J. Phys.: Condens. Matter **4**, 4323 (1992)
10. Romčević, N., Popović, Z.V., Khokhlov, D.R.: J. Phys.: Condens. Matter **7**, 5105 (1995)
11. Cochran, W., Cowley, R.A., Dolling, G., Elcombe, M.M.: Proc. Roy. Soc. A **293**, 433 (1966)
12. Miljković, J.M., Romčević, N., Popović, Z.V., König, W., Nikoforov, V.N.: Phys. Status Solidi (b) **193**, 43 (1996)
13. Pine, A.S., Dresselhaus, G.: Phys. Rev. B **4**, 356 (1971)
14. Steigmeier, E.F., Harbeke, G.: Solid State Commun. **8**, 1275 (1970)
15. Cape, J.A., Hale, L.G., Tennant, W.E. Surface Sci. **62**, 639 (1977)
16. Chang, I.F., Mitra, S.S.: Phys. Rev. **172**, 924 (1968); Genzel, L., Bauhofer, W.: Z. Phys. B **25**, 1 (1976)
17. Ravich, Yu.I., Efimova, B.A., Smirnov, I.A.: In: Stil'bans, L.S. (ed.) Semiconducting Lead Chalogenides. New York: Plenum Press 1970
18. Peterson, D.L., Petrow, A., Giriat, W., Ramdas, A.K., Rodriguez, S.: Phys. Rev. B **33**, 1160 (1986)
19. Volkov, B.A., Kusmin, V.P., Pankratov, O.A.: Fiz. Tverd. Tela **24**, 415 (1982)
20. Belogorokhov, A.I., Belokon', S.A., Ivanchik, I.I., Khokhlov, D.R.: Fiz. Tverd. Tela **34**, 1651 (1992) [Engl. Trans. Sov. Phys. Solid State **34**, 2966 (1992)]
21. Akimov, B.A., Brandt, N.B., Gas'kov, A.M., Zlomanov, V.P., Ryabova, L.I., Khokhlov, D.R.: Fiz. Tekh. Popuprovodn. **17**, 87 (1993) [Engl. Trans. Sov. Phys. Semicond. **17**, 53 (1983)]
22. de Viser, A., Ivanchik, I.I., Nikorich, A.V., Khokhlov, D.R.: to be published